

# A Comparison of the Amounts of Artifacts Produced by Five Cements in Cone-Beam CT

Mahkameh Moshfeghi,<sup>1</sup> Shadi Hamidiaval,<sup>2,\*</sup> Mohsen Pakghalb,<sup>3</sup> and Alireza Akbarzadeh Baghban<sup>4</sup>

<sup>1</sup>Department of Oral and Maxillofacial Radiology, Dental Faculty, Shahid Beheshti University of Medical Sciences, Tehran, IR Iran

<sup>2</sup>Department of Oral and Maxillofacial Radiology, Dental Faculty, Lorestan University of Medical Sciences, Khorramabad, IR Iran

<sup>3</sup>Faculty of Technical and Engineering, Science and Research Branch, Islamic Azad University, Tehran, IR Iran

<sup>4</sup>Department of Basic Sciences, School of Rehabilitation, Shahid Beheshti University of Medical Sciences, Tehran, IR Iran

\*Corresponding author: Shadi Hamidiaval, Department of Oral and Maxillofacial Radiology, Dental Faculty, Lorestan University of Medical Sciences, Khorramabad, IR Iran. Tel: +98-2188077784, Fax: +98-2122371485, E-mail: shadi\_h65@yahoo.com

Received 2015 February 07; Revised 2015 March 22; Accepted 2015 May 06.

## Abstract

**Background:** Bidimensional radiographic methods, including periapical, occlusal, panoramic, and cephalometric radiographs, are widely used in dentistry. However, the superimposition of adjacent structures and consequent loss of anatomic details may occur.

**Objectives:** The purpose of this study is to evaluate the artifacts produced by different cements with different densities using cone-beam computed tomography (CBCT).

**Materials and Methods:** Samples of five cements with different densities including glass ionomers (or GI, from ChemFil Rock and Fuji IX), mineral trioxide aggregates (MTA), zinc oxide eugenol (ZOE), TempBond and a control sample (polyester) were scanned by CBCT device and analyzed using OnDemand 3D application software. The amount of artifacts was measured by  $\Delta$  gray scale value ( $\Delta$ GSV), which was achieved by subtracting the gray level of the samples from the control group.

**Results:** According to the mean GSV of the five different materials, the majority of artifacts produced were as follows: TempBond > ZOE > MTA > GI (ChemFil Dentsply) > GI (GC, Fuji IX).

**Conclusions:** The type of materials can influence the obtained GSV. Different materials cause various amounts of artifacts due to differences in density and atomic number.

**Keywords:** Artifacts, Cone-Beam Computed Tomography, Dental Cements

## 1. Background

Bidimensional radiographic methods, including periapical, occlusal, panoramic and cephalometric radiographs, are widely used in dentistry (1). However, the superimposition of adjacent structures and consequent loss of anatomic details may occur (1). To overcome these disadvantages, computed tomography (CT), has been employed in dentistry for the diagnosis of soft and hard tissue lesions since 1978 (2). By this method, more precise quantitative and qualitative evaluation of adjacent structures is possible. However, application of CT scan in dental procedures has some disadvantages, including high costs, large equipment size, image artifacts and high radiation doses (3, 4). Since 1990, the development of cone-beam computed tomography (CBCT) has become a very important alternative diagnostic tool for overcoming these drawbacks (1, 2). CBCT is now used for treatment planning in endodontic surgery, airway assessment, orthodontics, and evaluation of pathological lesions to provide three-dimensional images (2). It is a less complex device that produces images

with satisfactory resolution, with low artifact incidence and a lower dose of radiation (5-7). Several studies have shown that CBCT provides precise linear measurements of dentomaxillofacial structures (8, 9). Artifacts are known as image quality degradation factors in both CT and CBCT scanning (4). Artifacts are caused by abrupt transitions between low and high-density materials, which result in data values that exceed the dynamic range of the processing electronics (10). Since metallic objects in a human body have much higher attenuation coefficients than that of soft tissue and produce annoying artifacts such as streak and shade artifacts (3,7), artifact reduction has been a problem in cone-beam CT imaging. These artifacts significantly degrade the visual quality of the images, and they distort the images of skeletal structures close to metallic objects. The two main sources of metal artifacts are photon starvation and beam hardening. Many studies have evaluated the artifacts induced by metals in CBCT imaging systems (10-12). Gray level is a calibrated sequence of gray tones, ranging from black to white. These are the digital numbers of each of the pixel units that together make up a remotely

sensed frame (13). Some arbitrariness in values exists, particularly when related to the X-ray beam hardening effect, scattered radiation, changes in the volume of the field of view (FOV), and the exposure conditions (KVP and mA) (14). Several methods have explored to reduce metal artifacts in CBCT imaging (15-18).

## 2. Objectives

Knowledge of the ingredients in dental materials will help manufacturers to produce materials that induce fewer artifacts in CBCT imaging and maintain favorable physical properties. There have been few studies aimed at evaluating the artifacts induced by endodontic and restorative materials in CBCT imaging. Therefore, the purpose of the present study is to evaluate the gray scale value of selected dental materials in CBCT scanning.

## 3. Materials and Methods

### 3.1. Specimen Preparation

In this descriptive-analytic study, holes measuring 3 mm in diameter and 2 mm in height were fabricated in polyester molds ( $n = 1$ ). GI ChemFil Rock Dentsply (Konstanz, Germany), ZOE (S.S. White Dental manufacturing Co., Philadelphia), MTA ProRoot Dentsply (Konstanz, Germany), GI (GC, Fuji IX, GC Europe N.V, Leuven, Belgium) and TempBond (Kerr manufacturing Co., Detroit, Michigan) were prepared according to the manufacturers' instructions and placed in molds. Additionally, a polyester mold without material served as a control sample. The components, and information about the materials, are listed in Table 1.

### 3.2. Scanning Procedure

Specimens were scanned using the NewTom VGI (AFP imaging company, 2010) CBCT scanner. The CBCT scanner was operated at  $\text{mA} = 4$ ,  $\text{kVp} = 110$ , with  $\text{FOV} 8 \times 8$  cm. The acquired data were reconstructed with 2 mm axial slice thickness. An example of CBCT image is shown in figure 1.

### 3.3. Image Analysis

The images, in DICOM format, were imported into the OnDemand 3D application. Using tools in the software, a circular region of interest (ROI) 1 cm in diameter was chosen. In the next step, the gray scale value of the ROI was measured at three locations, 1, 2 and 4 mm from the outline of the dental material, which were 2.5, 3.5 and 5.5 mm away from the center of the sample, respectively, and in four directions (a, b, c and d). This is demonstrated in schematic view in Figure 2. The GSV was measured in a series of four

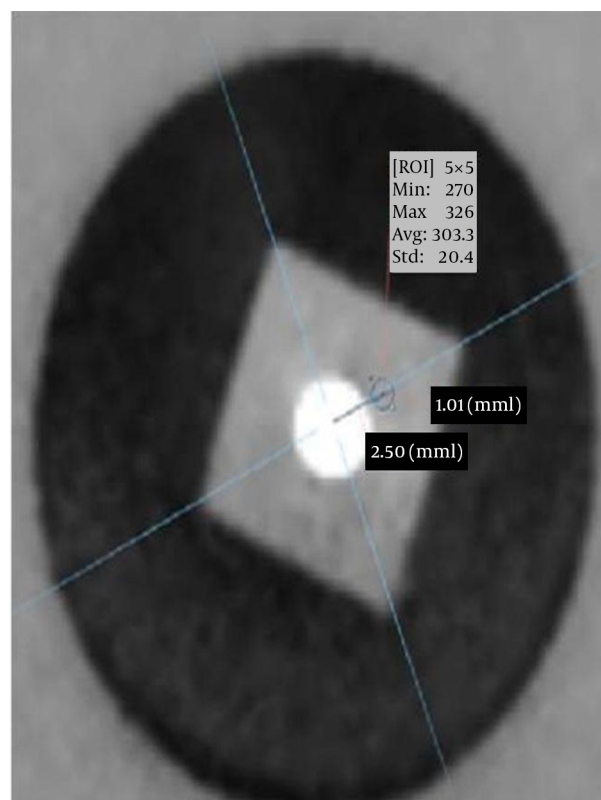


Figure 1. Image of the Scanned Material in the CBCT Device

numbers including minimum, maximum, standard deviation and average (Figures 3 and 4). Two oral radiologists served as observers. The revision was done randomly by the expert one to eliminate observer error.

### 3.4. Statistical Analysis

The collected data were entered in statistical package for the social sciences version 16 (SPSS Inc., Chicago, Illinois). Mean, standard deviation, minimum and maximum were descriptive data which were used for artifact measurement. The values of the GSVs of the materials were subtracted from the values of the control material at all three locations and in all four directions in order to achieve the  $\Delta\text{GSV}$ . Descriptive statistical analysis was performed on the  $\Delta\text{GSV}$  for each of the dental materials.

## 4. Results

The  $\Delta\text{GSV}$  for TempBond was in average 410 and was more than the other tested materials. The second greatest delta was ZOE, with an average of 395.25, followed by MTA, with an average of 281.5. The glass ionomers had the

**Table 1.** Information About the Dental Materials in the Samples

Material	Components	Manufactures
TempBond	Zinc Oxide	Kerr Manufacturing Co. Detroit, Michigan
GI ChemFil Rock	Calcium, Aluminum, Fluoru, Iron, Phosphor	Dentsply Konstanz, Germany
ZOE	Eugenol, Zinc Oxide, Zinc Stearate, White Rosin, Zinc Acetate	(S.S. White Dental Manufacturing Co., Philadelphia)
MTA ProRoot	Sio2, Calcium Oxide, Magnesium Oxide, K2So4	Dentsply Konstanz, Germany
GI GC, Fuji IX	Silicate Glass, Aluminum, Fluoru, Polyacrylic Acid	GC Europe N.V, Leuven, Belgium

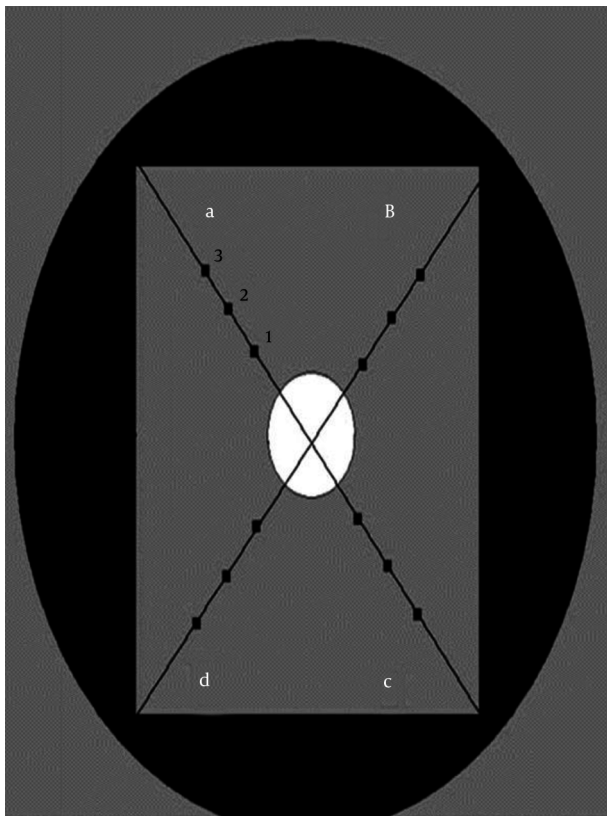
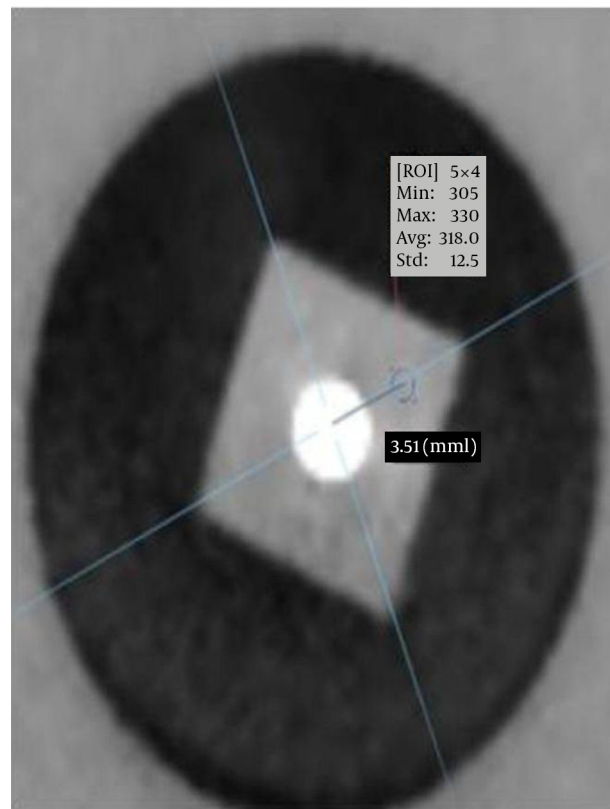


**Figure 2.** A Schematic View Showing the Selection of Three Locations and Four Directions for Measuring GSV

lowest delta values. The mean value for the ChemFil Rock was 197.4, which was greater than the 92.75 delta of the Fuji IX. Additionally, we evaluated the influences of the location and direction of the ROI in the material on artifact production. The maximum deviation of the values in comparison with the values of the control sample was seen at the location closest to the outline of the dental material 1 mm from the center. For values of ChemFil at 1 mm location, the average was 197.37, 165.12 at 2 mm and 121.62 at the last location. For ZOE, these values were measured to be 395.30,

**Figure 3.** Measuring the Gray Value at the ROI

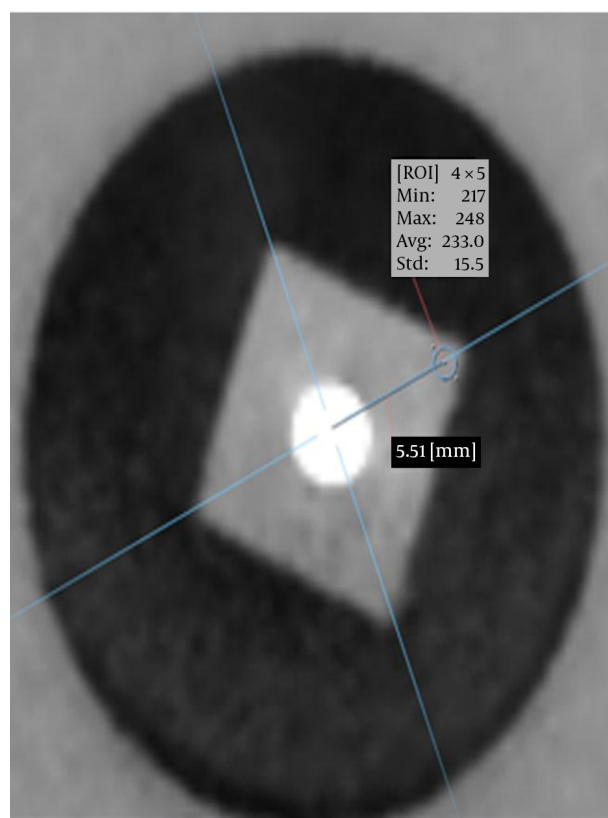


This is a circle in 1 mm away from the outline of the material in the b2 direction

158.45, and 118.1, respectively. For MTA, the average values measured at the three locations were 281.5, 162.6, and 136.9. The values for Fuji IX were 92.75, 55, and 38.75, respectively. The influence of the direction of the ROI on measurements of the gray level values was unclear, as the uniformity in distributions of values among the four directions was distinct. For example, in ChemFil, the mean value of the  $\Delta$ GSV in direction a, was 148, in direction b, 144, in direction c, 143 and in direction d, 130. None of which were statistically different. The results are shown in Table 2.

**Table 2.** Average  $\Delta$ GSV of Each Sample in Three Locations and Four Directions

Direction and Distance	GI ChemFil Dentsply	MTA	ZOE	GI (GC, Fuji II )	TempBond
a1	200.2	231.6	325	153	328
a2	190	97	165.5	95.5	168
a3	180	66.5	22.5	44.5	30
b1	131	294	320	94.5	310
b2	128	188	162.5	33	170
b3	102	177.7	158	30.5	153
c1	193	249	350	105	354
c2	145	167.4	108.5	73.5	210
c3	95.9	132.4	97.4	63	115
d1	265.5	351.7	285.5	18.5	290
d2	197.5	198	197.3	18	198
d3	109	171	194.5	17	193

**Figure 4.** Measuring the Gray Value at the ROI

This is a circle 1 mm away from the outline of the material in the b3 direction.

## 5. Discussion

In the present study, we used the NewTom VGI 2010 CBCT system and the OnDemand3D application software for determination of GSV of different materials. The long-term use of different restorative materials in dentistry necessitates evaluation of artifacts produced in the oral cavity by three-dimensional systems. A number of studies have evaluated the artifacts in CBCT imaging, their description, causes and reduction algorithms (12, 15, 18), but a little has been done on various dental materials. Chindasombatjareon et al. evaluated the metallic artifacts produced by cubes of titanium in CT and CBCT (19). Esmaeili et al. performed a study on artifacts produced by titanium dental implants in various imaging systems with different kVp selection parameters. They concluded that the difference in artifact production can be attributed to the difference in the amount of X-ray penetration, and that higher values of kVp result in fewer artifacts being observed (4). In our study, we evaluated artifacts induced by different dental materials with different densities using the same scanning parameters. The difference in the amount of X-ray absorption in different materials depending on their atomic number and densities led to different amounts of induced artifacts. Our results were in accordance with the Chindasombatjareon and Esmaeili studies. In the current study, materials with higher atomic number, such as zinc and calcium, resulted in many more artifacts than materials with lower atomic number, such as hydrogen. This was in agreement with the result of Zhang [U+02BC]s study. They observed more artifacts produced by silver points in comparison with gutta-percha, due to its higher atomic number (20). We also concluded that the materials with higher

atomic numbers lead to more beam-hardening artifacts. Kuusisto et al. assessed the amount of beam-hardening artifacts in titanium and zirconium implants and resin-BaAlSiO<sub>2</sub> simulated implants under CBCT scanning. They utilized the ImageJ software application for analyzing gray values. They observed strong artifact production in CBCT images from titanium and zirconium, and composite materials which consisted of at least 20% BaAlSiO<sub>2</sub>. The intensity of artifacts increased as the radio-opacity of the composite material increased (21). The samples used in this study had the same geometric shapes and dimensions, thus, differences in the amount of artifacts due to the difference in structural elements eliminated. Draener et al. evaluated the amounts of artifacts in three plans of reconstructions. The observations were all done in axial, coronal and three-dimensional reformatted images. The ability to demonstrate the intensity of the artifact was the same. Additionally, they concluded that increasing the distance from the center of the FOV resulted in an increase in radial-shaped artifact production (22). The present results showed radial-shaped artifacts due to the round shape of samples.

### 5.1. Conclusion

From the results described above, we determined that TempBond had the highest amount of artifact production, in comparison with four other base materials, due to its density and atomic number. Fuji IX glass ionomer showed the lowest amount of the beam hardening artifact. Thus, using the material with lower density and atomic number leads to less X-ray absorption and fewer artifacts in the final images. The small number of samples was the limitation of this study, which acts as the basic data for further investigation. We also suggest further investigation is needed on gray level values, its determinants and accuracy among different CBCT machines.

### Acknowledgments

The authors would like to thank Dr. Yaser Safi for his cooperation in sample preparation.

### Footnotes

**Authors' Contribution:** Study concept and design: Mahkameh Moshfeghi; acquisition of data: Shadi Hamidiaval; analysis and interpretation of data: Mohsen Pakghalb, and Shadi Hamidiaval; drafting of the manuscript: Mohsen Pakghalb; critical revision of the manuscript for important intellectual content: Shadi Hamidiaval, and Mahkameh Moshfeghi; statistical analysis: Alireza Akbarzadeh Baghban.

**Funding/Support:** This study was part of a post-doctoral thesis by Dr. Shadi Hamidiaval under the supervision of Dr. Mahkameh Moshfeghi. It was approved by the dental research center of Shahid Beheshti University of Medical Sciences, school of dentistry.

### References

- White SC, Pharoah MJ. Oral radiology: Principles and interpretation. Elsevier Health Sciences; 2014.
- Hanrahan NP, Stuart GW, Delaney KR, Wilson C, Psychiatric/Mental Health Expert P. Mental health is an urgent public health concern. *Nurs Outlook*. 2013;**61**(3):185–6. [PubMed: 23814796].
- Barrett JF, Keat N. Artifacts in CT: recognition and avoidance. *Radiographics*. 2004;**24**(6):1679–91. doi: 10.1148/rg.246045065. [PubMed: 15537976].
- Esmaili F, Johari M, Haddadi P. Beam hardening artifacts by dental implants: Comparison of cone-beam and 64-slice computed tomography scanners. *Dent Res J*. 2013;**10**(3):376.
- Scarfe WC, Farman AG, Sukovic P. Clinical applications of cone-beam computed tomography in dental practice. *J Can Dent Assoc*. 2006;**72**(1):75–80. [PubMed: 16480609].
- Hashimoto K, Arai Y, Iwai K, Araki M, Kawashima S, Terakado M. A comparison of a new limited cone beam computed tomography machine for dental use with a multidetector row helical CT machine. *Oral Surg Oral Med Oral Pathol Oral Radiol Endod*. 2003;**95**(3):371–7. doi: 10.1067/moe.2003.120. [PubMed: 12627112].
- Loubele M, Maes F, Jacobs R, van Steenberghe D, White SC, Suetens P. Comparative study of image quality for MSCT and CBCT scanners for dentomaxillofacial radiology applications. *Radiat Prot Dosimetry*. 2008;**129**(1-3):222–6. doi: 10.1093/rpd/ncn154. [PubMed: 18583372].
- Lasca CA, Panella J, Marques MM. Analysis of the accuracy of linear measurements obtained by cone beam computed tomography. *Eur Radiol*. 2004;**33**(5):291–4. doi: 10.1259/dmfr/25500850.
- Moshfeghi M, Tavakoli MA, Hosseini ET, Hosseini AT, Hosseini IT. Analysis of linear measurement accuracy obtained by cone beam computed tomography (CBCT-NewTom VG). *Dent Res. J*. 2012;**9**(Suppl 1):S57.
- Katsumata A, Hirukawa A, Noujeim M, Okumura S, Naitoh M, Fujishita M, et al. Image artifact in dental cone-beam CT. *Oral Surg Oral Med Oral Pathol Oral Radiol Endod*. 2006;**101**(5):652–7. doi: 10.1016/j.tripleo.2005.07.027. [PubMed: 16632279].
- Esmaili F, Johari M, Haddadi P, Vatankhah M. Beam hardening artifacts: comparison between two cone beam computed tomography scanners. *Dent Res J*. 2012;**6**(2):49.
- Schulze RK, Berndt D, d'Hoedt B. On cone-beam computed tomography artifacts induced by titanium implants. *Clin Oral Implants Res*. 2010;**21**(1):100–7. doi: 10.1111/j.1600-0501.2009.01817.x. [PubMed: 19845706].
- Mah P, Reeves TE, McDavid WD. Deriving Hounsfield units using grey levels in cone beam computed tomography. *Oral Surg Oral Med Oral Pathol*. 2014;**39**(6):323–35.
- Parsa A, Ibrahim N, Hassan B, Stelt P, Wismeijer D. Bone quality evaluation at dental implant site using multislice CT, micro-CT, and cone beam CT. *CLIN ORAL IMPLAN RES*. 2015;**26**(1):e1–7.
- Meilinger M. Metal artifact reduction and image processing of cone-beam computed tomography data for mobile C-arm CT devices. University of Regensburg; 2011.
- Bechara BB, Moore WS, McMahan CA, Noujeim M. Metal artefact reduction with cone beam CT: An in vitro study. *Oral Surg Oral Med Oral Pathol*. 2014;**41**(3):248–53.

17. Meilinger M, Schmidgunst C, Schutz O, Lang EW. Metal Artifact Reduction in CBCT Using Forward Projected Reconstruction Information and Mutual Information Realignment. Springer;. 2009. pp. 46–9.
18. Bechara B, McMahan CA, Geha H, Noujeim M. Evaluation of a cone beam CT artefact reduction algorithm. *Oral Surg Oral Med Oral Pathol.* 2012;**41**(5):422–8. doi: [10.1259/dmfr/43691321](https://doi.org/10.1259/dmfr/43691321). [PubMed: [22362221](https://pubmed.ncbi.nlm.nih.gov/22362221/)].
19. Chindasombatjaroen J, Kakimoto N, Murakami S, Maeda Y, Furukawa S. Quantitative analysis of metallic artifacts caused by dental metals: comparison of cone-beam and multi-detector row CT scanners. *Oral Surg. Oral Med. Oral Pathol.* ;**27**(2):116–20. doi: [10.1007/s11282-011-0071-z](https://doi.org/10.1007/s11282-011-0071-z).
20. Zhang W, Makins SR, Abramovitch K. Research Article Cone Beam Computed Tomography (CBCT) artifact characterization of root canal filling materials. *J Investigative Dent.* 2014;**1**(1).
21. Kuusisto N, Vallittu PK, Lassila LVJ, Huuononen S. Evaluation of intensity of artefacts in CBCT by radio-opacity of composite simulation models of implants in vitro. *Oral Surg Oral Med Oral Pathol.* 2014;**44**(2):20140157.
22. Draenert FG, Coppentrath E, Herzog P, Muller S, Mueller-Lisse UG. Beam hardening artefacts occur in dental implant scans with the NewTom cone beam CT but not with the dental 4-row multidetector CT. *Oral Surg Oral Med Oral Pathol.* 2007;**36**(4):198–203. doi: [10.1259/dmfr/32579161](https://doi.org/10.1259/dmfr/32579161). [PubMed: [17536086](https://pubmed.ncbi.nlm.nih.gov/17536086/)].